Supporting Information

Thermal Evaporating-Trapping Strategy to Synthesize Flexible and Robust Oxygen Electrocatalysts for Rechargeable Zinc-Air Batteries

Hong-Bo Zhang[1], Yu Meng[2], Lingzhe Fang[3], Fei Yang[4], Shangqian Zhu[4], Tao Li[3, 5], Xiaohua Yu[6], Ju Rong[6],* Weiwei Chen[7], Dong Su[7],Yi Mei[1], Peng-Xiang Hou[2], Chang Liu[2],* Minhua Shao[4, 8],* Jin-Cheng Li[1],*

[1]Faculty of Chemical Engineering, Yunnan Provincial Key Laboratory of Energy Saving in Phosphorus Chemical Engineering and New Phosphorus Materials, Kunming University of Science and Technology, Kunming 650500, China.

[2]Shenyang National Laboratory for Materials Science, Institute of Metal Research, Chinese Academy of Sciences, Shenyang 110016, China.

[3]Department of Chemistry and Biochemistry, Northern Illinois University, 1425 W. Lincoln Hwy., DeKalb, IL, 60115, United States.

[4]Department of Chemical and Biological Engineering, Hong Kong University of Science and Technology, Clear Water Bay, Kowloon, Hong Kong, China

[5]X-ray Science Division, Argonne National Laboratory, 9700 South Cass Avenue, Lemont, Illinois 60439, United States

[6]Fok Ying Tung Research Institute, Hong Kong University of Science and Technology, Guangzhou 511458, China

E-mail: JRong_kmust@163.com (J. Rong), cliu@imr.ac.cn (C. Liu), kemshao@ust.hk (M. Shao), or jinchengli@kust.edu.cn (J. Li)

Experimental methods

1. Material preparation

1.1. Preparation of nitrogen-doped carbon fiber cloth (NCFC)

Cotton cloth was cut into a specific shape and size, and then immersed and rinsed several times in a solution of deionized water and ethanol to remove surface impurities. Subsequently, the cotton cloth was placed in a thermostatic oven set at 60 ℃ to undergo thorough drying. The dried cotton cloth was positioned at the center of reactor inserted in a horizontal tubular furnace, and a NH_3 flow was introduced to the reactor. The furnace temperature increased from room temperature to 900 ℃ at a rate of 15 ℃ min^{-1} and then kept 900 ℃ for 30 minutes. Afterward, the NH_3 flow was replaced with an Ar flow and the furnace temperature was maintained 900 ℃ for 30 minutes once more. NCFC was obtained by collecting the sample when the furnace temperature decreased to room temperature and then acid leaching in hydrofluoric acid was performed to remove impurities.

1.2. Preparation of Co_xFe_yO/NCFC

0.75 mmol phenylphosphonic acid and 0.75 mmol ferric nitrate nonahydrate were added in 100 ml deionized water, and then ultrasonicated to achieve a uniform solution. Subsequently, a flexible NCFC substrate (~100 mg) was added in the solution with a stirring rate of 200 rpm for 1 h. Then, 0.375 mmol of cobalt nitrate hexahydrate was add to the solution and continuously stirred at 200 rpm for 1 h. Afterward, 2.0 g of urea was added to the above solution. After complete dissolution,

the entire mixture was transferred to a 250 ml hydrothermal autoclave for reaction at 180 °C for 48 h. Finally, the Co_xFe_yO/NCFC precursor was collected by washing with deionized water and anhydrous ethanol and drying in a thermostatic oven at 60 °.

1.3. Preparation of CoFe-NP||SA/NCFC

The obtained $CoFeO_x$/NCFC precursor was placed in a tubular furnace and subjected to high-temperature treatment under an Ar atmosphere at 700 °C. The heating rate was maintained at 10 °C min^{-1}, and the dwell time at 700 °C was 1 hour. After the furnace was cooled down to room temperature, flexible self-supported CoFe-NP||SA/NCFC material was collected.

2. Material Characterization

The obtained materials were characterized using scanning electron microscopy (SEM, Nova Nano SEM 430, operated at 10 kV), transmission electron microscopy (Tecnai F20, 200 kV; Titan Cubed Themis G2, 300 kV), X-ray photoelectron spectroscopy (XPS, Escalab 250, Al Kα), inductively coupled plasma mass spectrometry (ICP-MS, Perkin Elmer Optima 4300 DV), and X-ray diffraction (XRD, Rigaku Miniflex 600, 40 kV).

In-situ XPS measurements were performed in an ultrahigh-vacuum setup equipped with a nonmonochromatic Al X-ray source and a hemispherical electron analyzer (Phoibos 100, SPECS GMbH). The measurements were conducted using an analyzer pass energy of E_{pass}=13 eV and a source power of P = 300 W. All spectra were aligned to the carbon peak (284.6 eV). The test equipment was Thermo Scientific Escalab 250Xi.

XAS experiments were performed at beamline 12-BM-B of the Advanced Photon Source (APS) at the Argonne National Laboratory. The energy of the incident monochromatic X-rays was selected by using a water-cooled Si (111) double crystal monochromator. The X-ray beam size is 500 μm horizontal × 1000 μm vertical. The energy resolution (ΔE/E) and photon flux (photos/sec) are 2×10^{-5} and 1×10^{11} @ 12 keV. The metal foil was measured for energy calibration for each scan of the samples. All spectra were collected in fluorescence mode expect the metal foil. XAS data reduction and analysis were processed by Athena software.

3. Electrochemical measurements

Electrochemical measurements were performed on an electrochemical analysis station (CHI 700 E and CHI 760 E, CH Instruments, China) using a standard three-electrode cell. A graphite rod and an Ag/AgCl electrode in a saturated KCl solution served as the counter electrode and reference electrode, respectively. All potential values refer to that of a reversible hydrogen electrode (RHE). To prepare the common working electrode, 5.0 mg of each catalyst was ultrasonically dispersed in ethanol containing 0.05 wt% Nafion (1.0 ml) to form a concentration of 5.0 mg ml^{-1} catalyst ink. The catalyst ink was then coated on the surface of the glassy carbon disk for the RDE and RRDE tests. The catalyst loading was 0.6 mg cm^{-2} and the loading of commercial Pt/C and Ir/C catalysts is 0.1 mg cm^{-2} without specific instructions. The ORR/OER polarization curves were recorded with *iR* compensation function of workstation and the compensation resistance was ~29 Ω. For testing the ORR and OER activity of the CoFe-NP||SA/NCFC film, the film was cut into appropriate size

with an effective contact area of 0.2 cm^{-2} (0.24 mg) and then directly clamped by titanium sheet electrode, which was denoted as CoFe-NP||SA/NCFC(film). Simultaneously, the CoFe-NP||SA/NCFC catalyst ink coated on carbon cloth (0.2 cm^{-2}) with the same loading of 0.24 mg was used for comparison, referred to as CoFe-NP||SA/NCFC-700(powder). To enhance the diffusion of oxygen, the electrolytic cell was placed on a magnetic stirrer with a stirring speed of 600 rpm during the experimental measurements. The film-based ORR/OER polarization curves were also recorded with *iR* compensation function of workstation and the compensation resistance was ~50 Ω.

For the RRDE tests, the polarization curves were collected at disk rotation rates of 1600 rpm. The scan rate was 5 mV s^{-1} and the potential of ring was set at 0.3 V (vs. Ag/AgCl). The collecting efficiency of the RRDE (N) was 0.37. The peroxide yield (HO_2^- %) and the electron transfer number (n) was calculated as follows:

$$HO_2^- \% = 200 \times \frac{I_r / N}{I_d + I_r / N}$$

$$n = 4 \times \frac{I_d}{I_d + I_r / N}$$

where I_d is the disk current and I_r is the ring current.

The durability of ORR and OER was evaluated by testing the linear scan voltammogram of CoFe-NP||SA/NCFC modified electrodes at 1600 rpm before and after 5000 continuous cyclic voltammetry (CV) potential cycles.

4. ZAB tests

4.1. Liquid-state ZABs

A polished zinc plate was used as the anode and a mixed solution of KOH (6.0 mol L^{-1}) and $Zn(CH_3COO)_2$ (0.2 mol L^{-1}) was used as the electrolyte. Ni foam (current collector), CoFe-NP||SA/NCFC film, and hydrophobic carbon cloth (gas diffusion layer) were assembled by simply compressing to act as the air cathode. The reserved active window area was 1 cm^2. CoFe-NP||SA/NCFC film catalyst loading was 1.2 mg cm^{-2}. All the liquid-state ZAB performances were tested in an air atmosphere.

For comparison, CoFe-NP||SA/NCFC (loading: 1.2 mg cm^{-2}) and mixed Pt/C+Ir/C (loading: 0.2 mg cm^{-2}) catalyst inks were coated on hydrophobic carbon clothes. Subsequently, the catalyst-modified carbon cloth together with Ni foam were assembled by simply compressing to act as the air cathode. The reserved active window area was also 1 cm^2.

4.2. Solid-state ZABs

Homemade solid-state ZABs were assembled using a polished zinc plate as the anode, gel as the electrolyte, CoFe-NP||SA/NCFC film as both the catalyst layer and gas diffusion layer, and Ni foam as the current collector. For the gel electrolyte preparation, 30 mg of graphene oxide (GO) was dispersed in 10 ml of deionized water and sonicated for homogenization. Subsequently, 1 g of polyvinyl alcohol (PVA) was dissolved in 20 ml of deionized water with vigorous stirring at 95 °C. The GO solution was then added to the PVA solution and mixed thoroughly. Next, 9.5 ml of acrylic acid ($C_3H_4O_2$) was added, followed by neutralization using 11 ml of 8.4 M sodium hydroxide (NaOH). Subsequently, 0.025 g of N, N'-Methylenebisacrylamide (MBA) and 5 ml of 0.15 M potassium persulfate ($K_2S_2O_8$) were added. The mixture

was stirred for 30 minutes and then allowed to solidify at 70°C for 3 h. Afterward, the solid was soaked in a 4 M potassium hydroxide (KOH) solution for approximately 15 h before use. Catalyst loading for solid-state ZABs was the same as that for liquid-state ZABs. All the solid-state ZAB performances were tested in an air atmosphere.

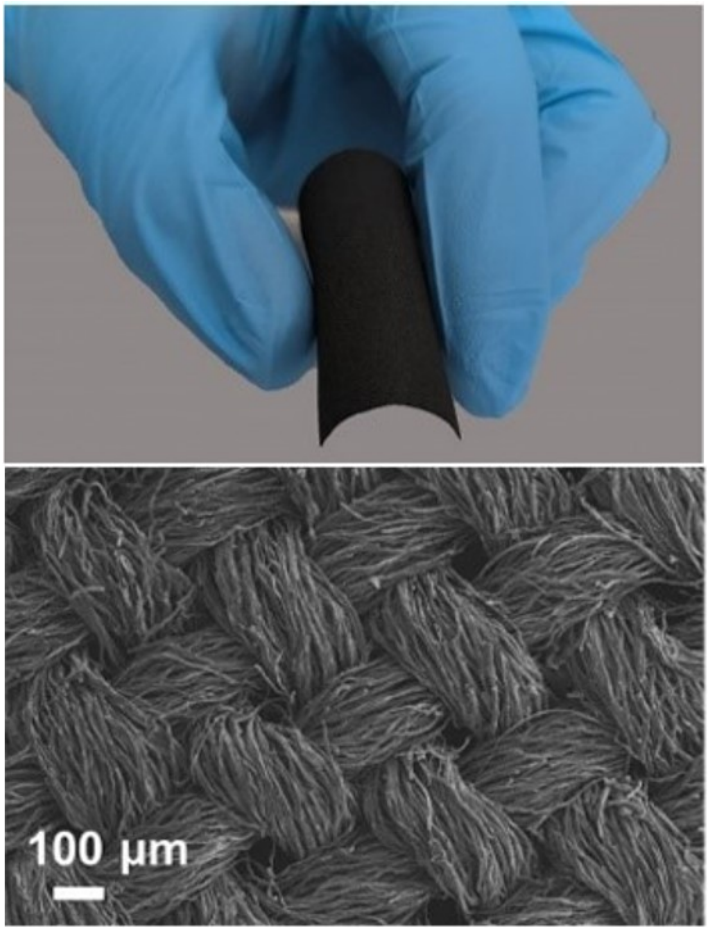

Figure S1. (a) Optical photograph of NCFC showing its good flexibility. (b) SEM image showing the woven fiber-like structure of NCFC.

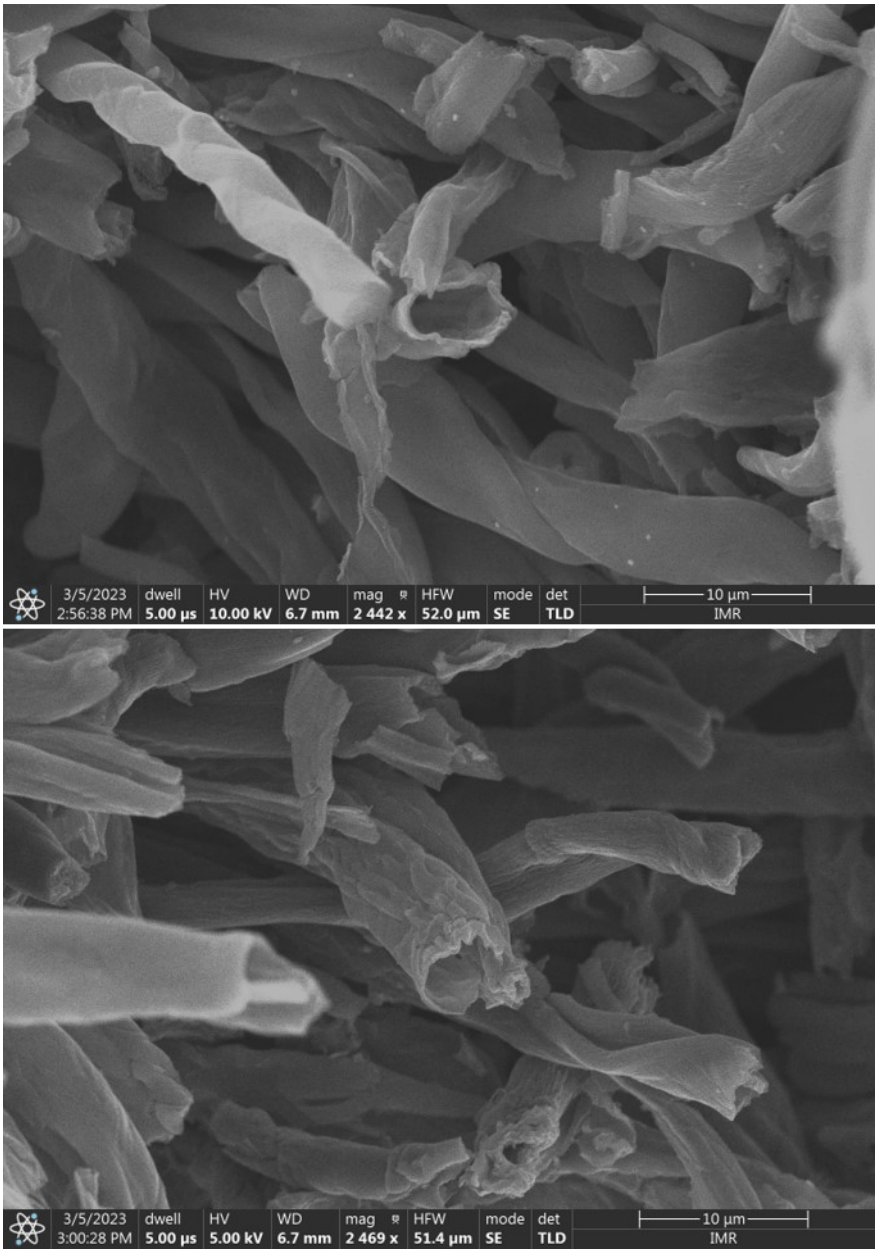

Figure S2. SEM images of the obtained NCFC showing the hollow tubular structure of composing fibers.

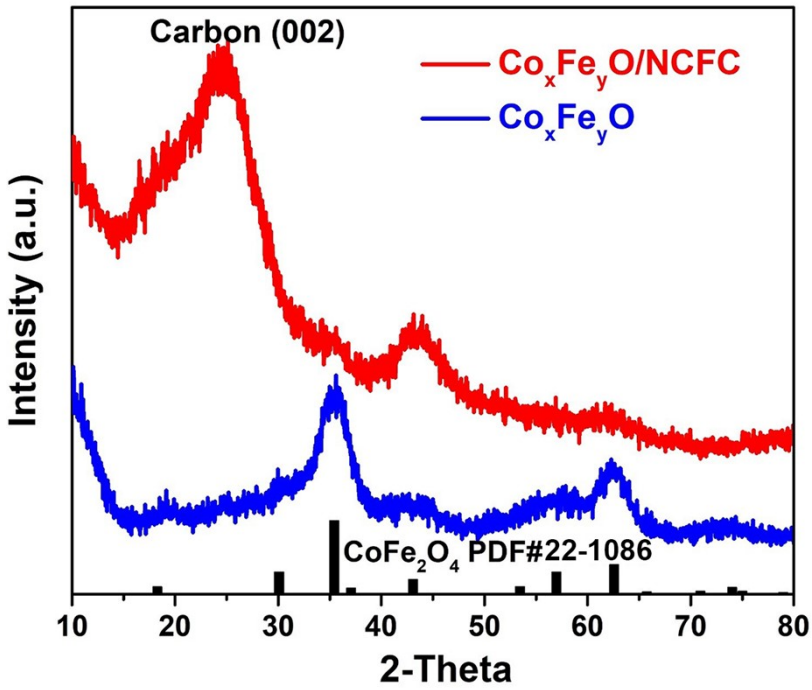

Figure S3. XRD pattern of Co_xFe_yO/NCFC and reference sample of Co_xFe_yO prepared in the absence of NCFC.

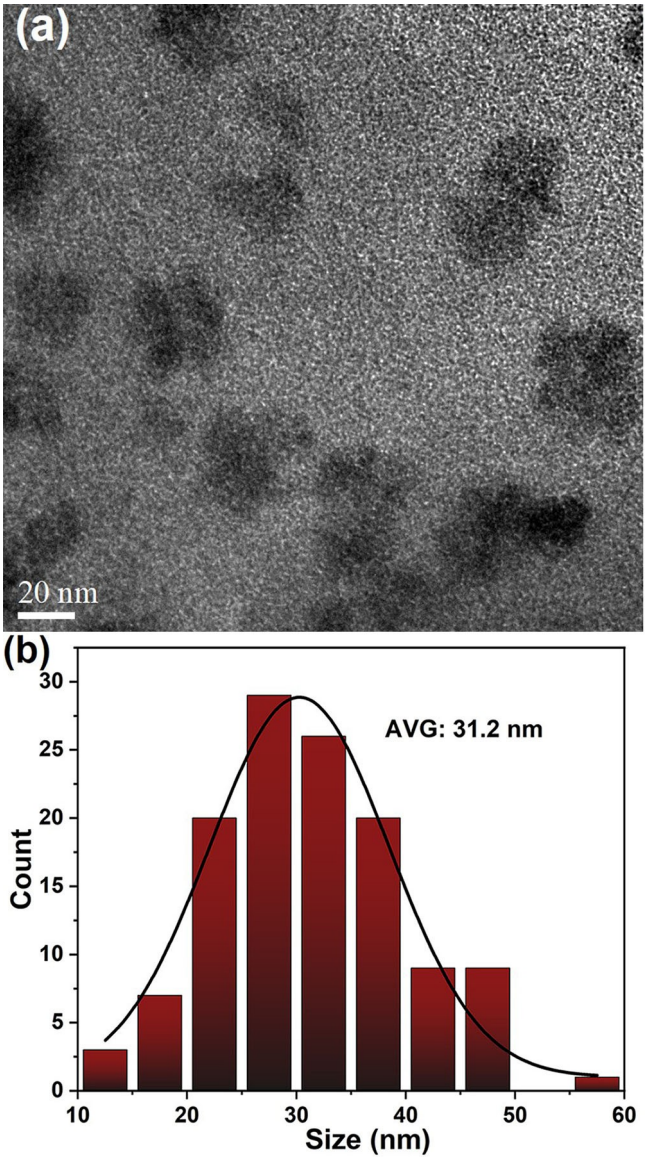

Figure S4. (a) A typical TEM image of Co_xFe_yO/NCFC. (b) Chart showing the size distribution of Co_xFe_yO in Co_xFe_yO/NCFC.

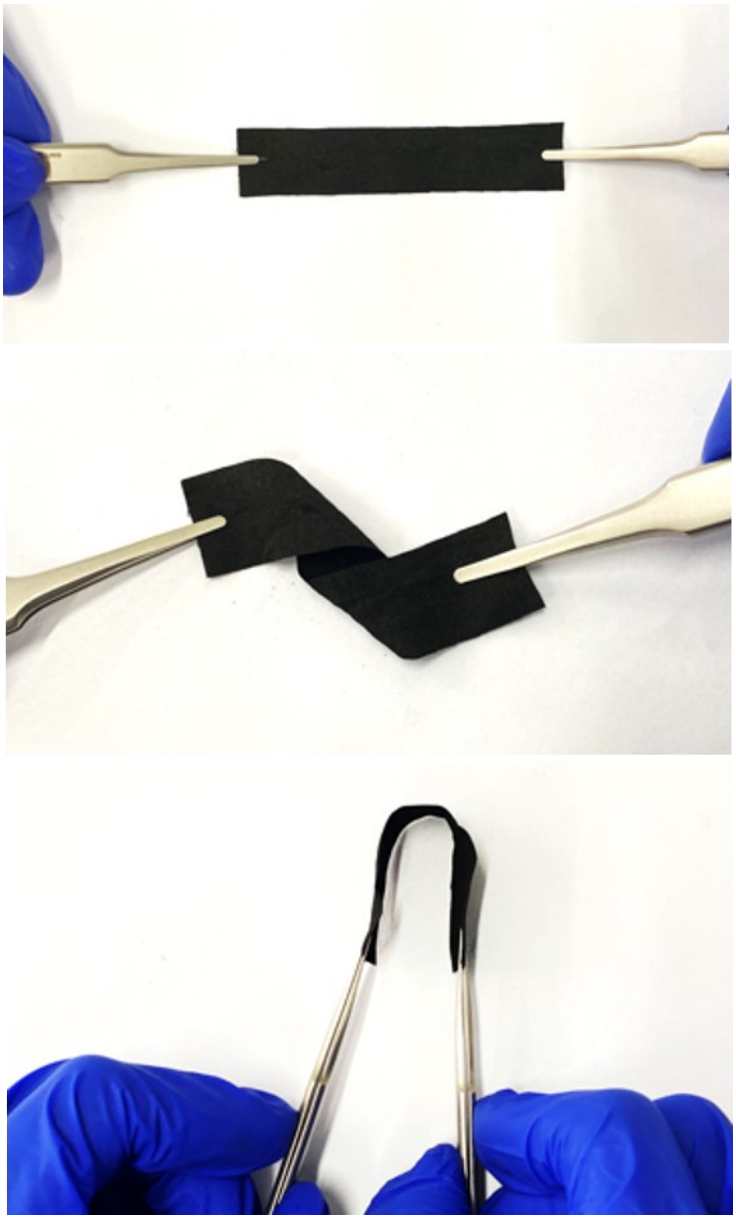

Figure S5. Optical photographs showing the good flexibility of CoFe-NP||SA/NCFC.

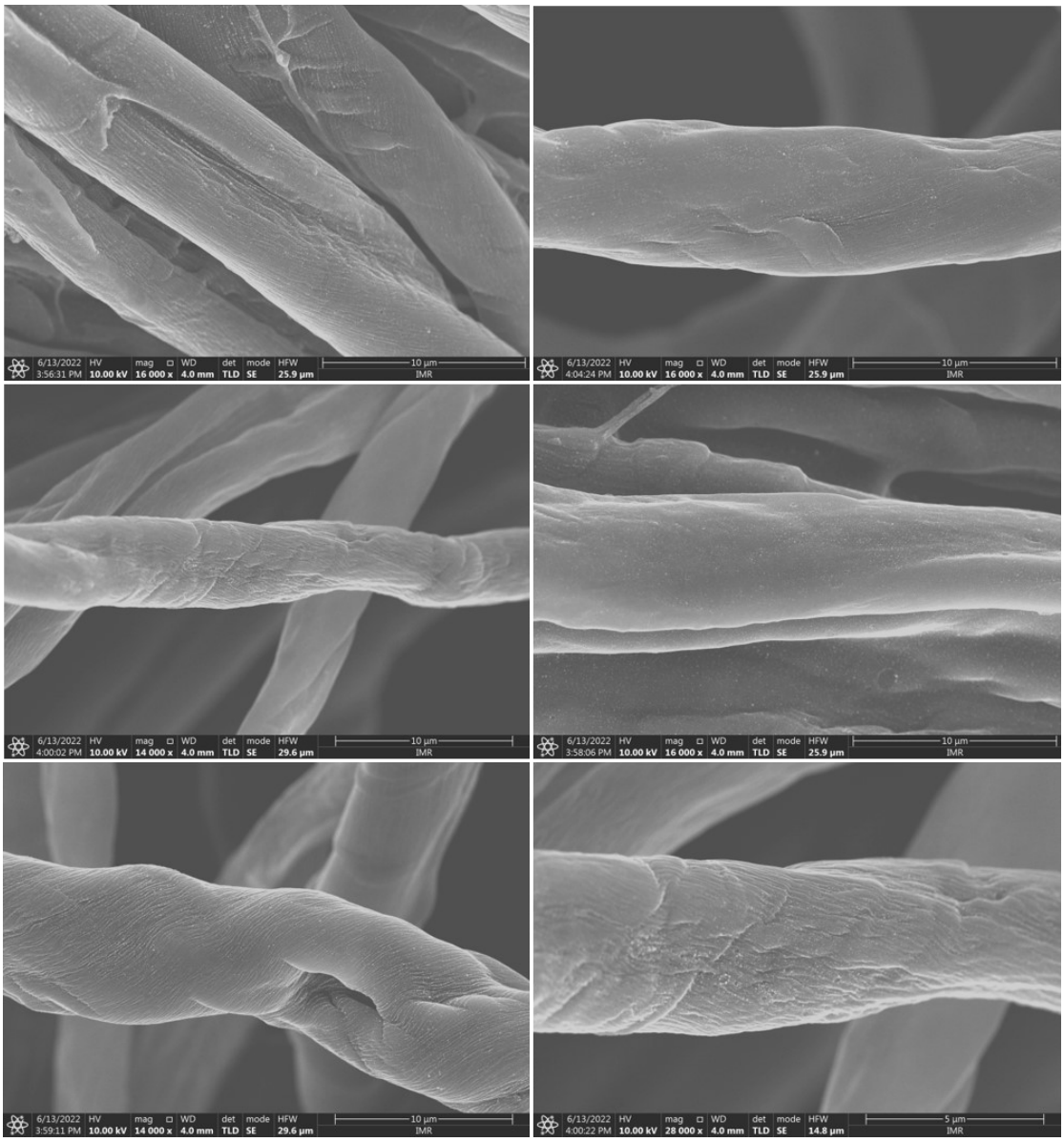

Figure S6. SEM images of CoFe-NP||SA/NCFC.

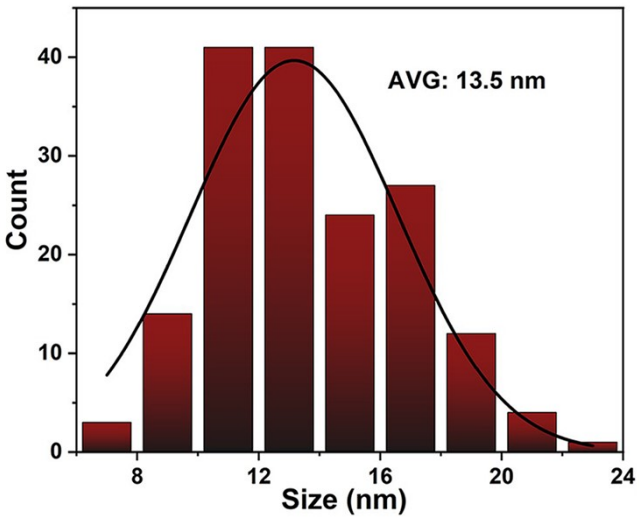

Figure S7. Chart showing the size distribution of CoFe nanoparticles in CoFe-NP||SA/NCFC.

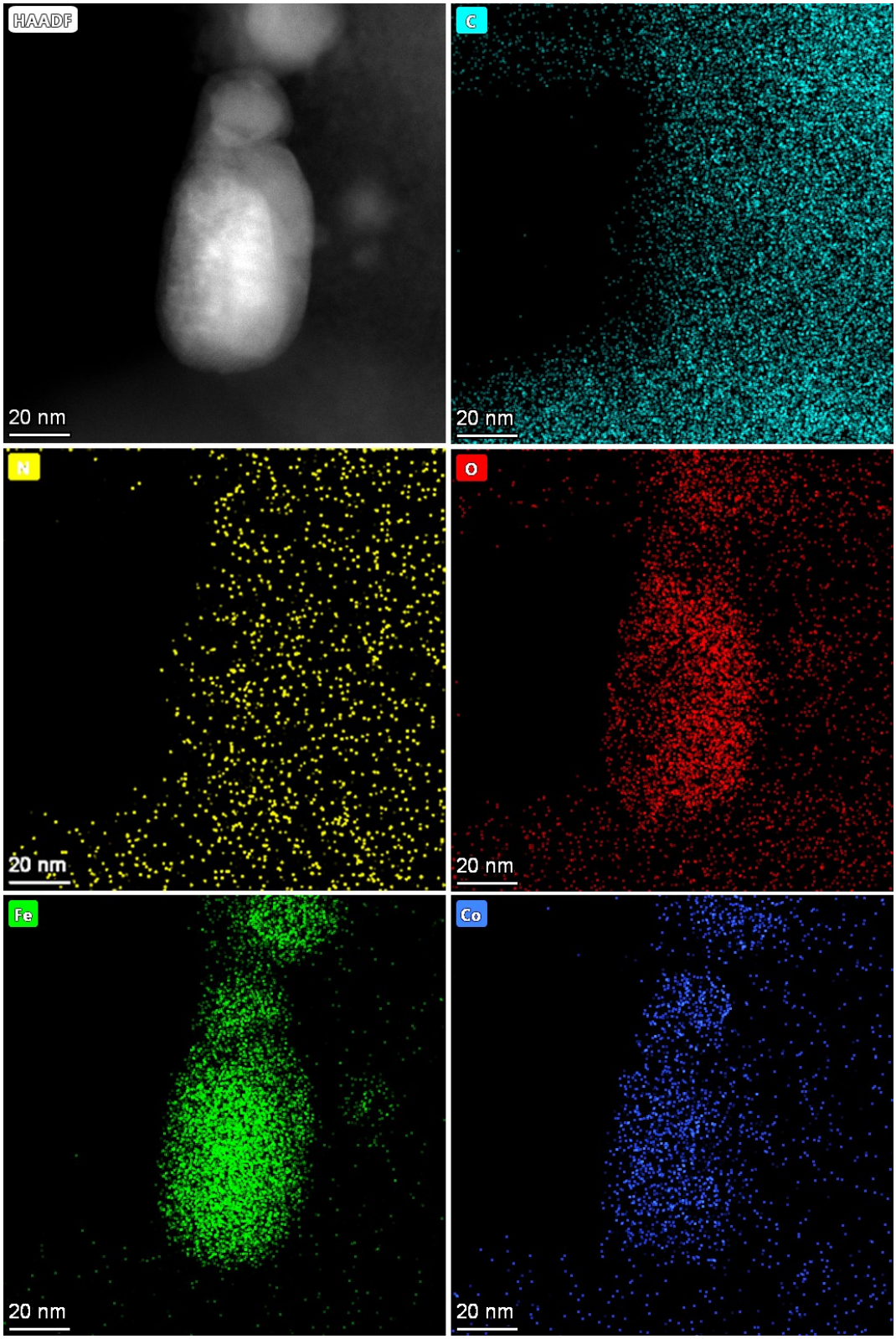

Figure S8. STEM imaging and the corresponding element mapping of CoFe-NP||SA/NCFC.

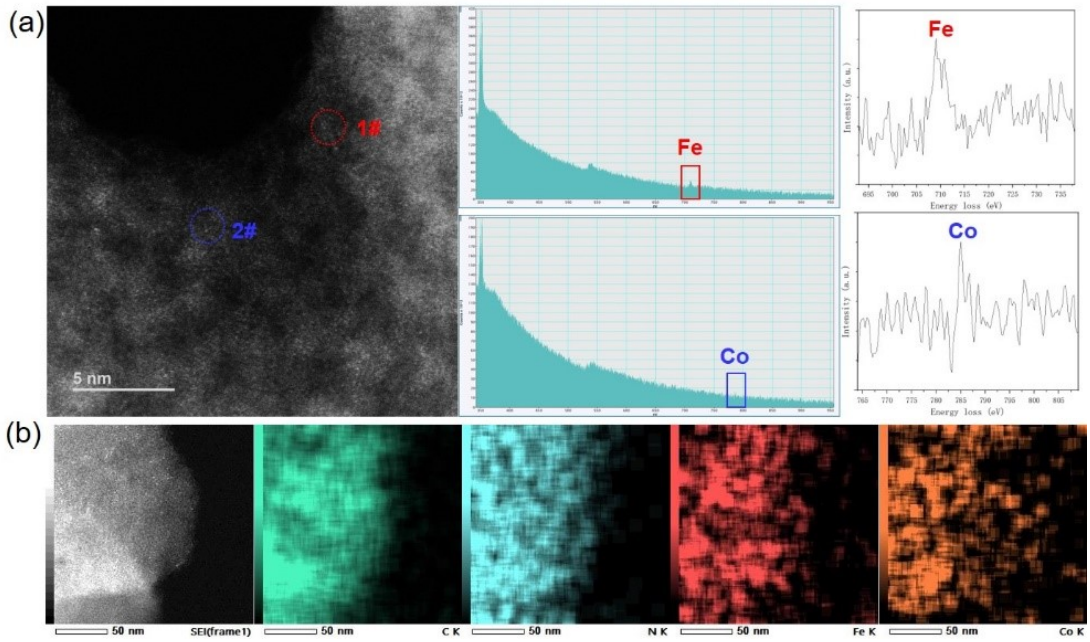

Figure S9. (a) HAADF-STEM image and corresponding EELS analysis to verify the coexistence of Co and Fe at the atomic level in CoFe-NP||SA/NCFC. (b) HAADF-STEM image and corresponding EDS element mappings.

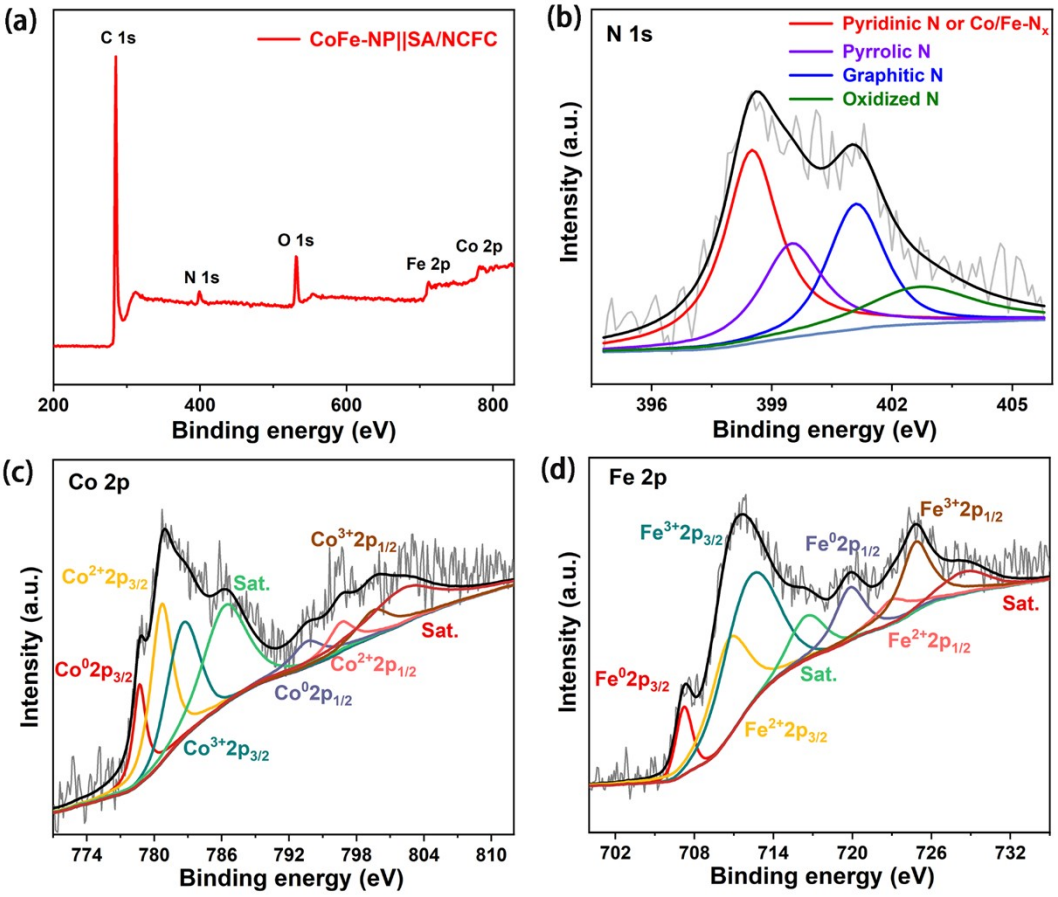

Figure S10. XPS spectra of CoFe-NP||SA/NCFC.

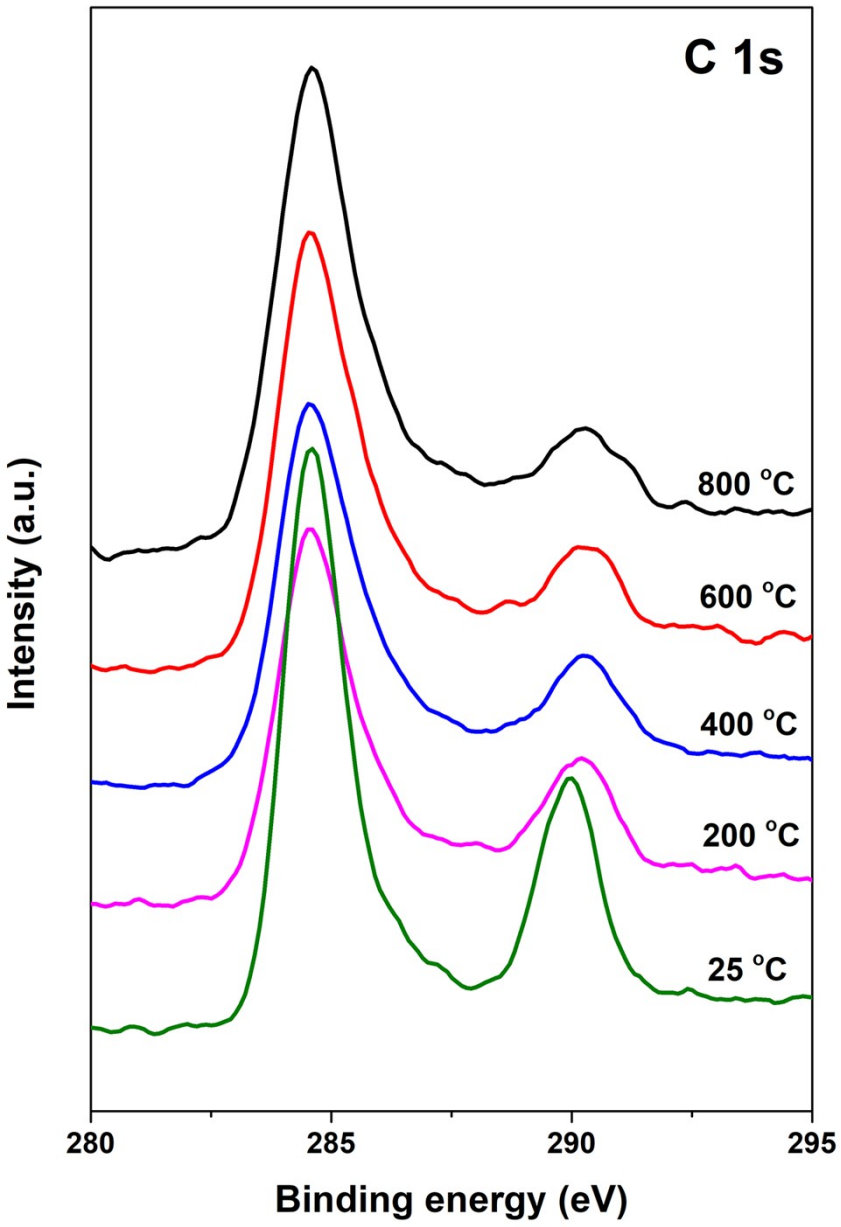

Figure S11. *In-situ* XPS C 1s spectra recorded during the preparation of CoFe-NP||SA/NCFC.

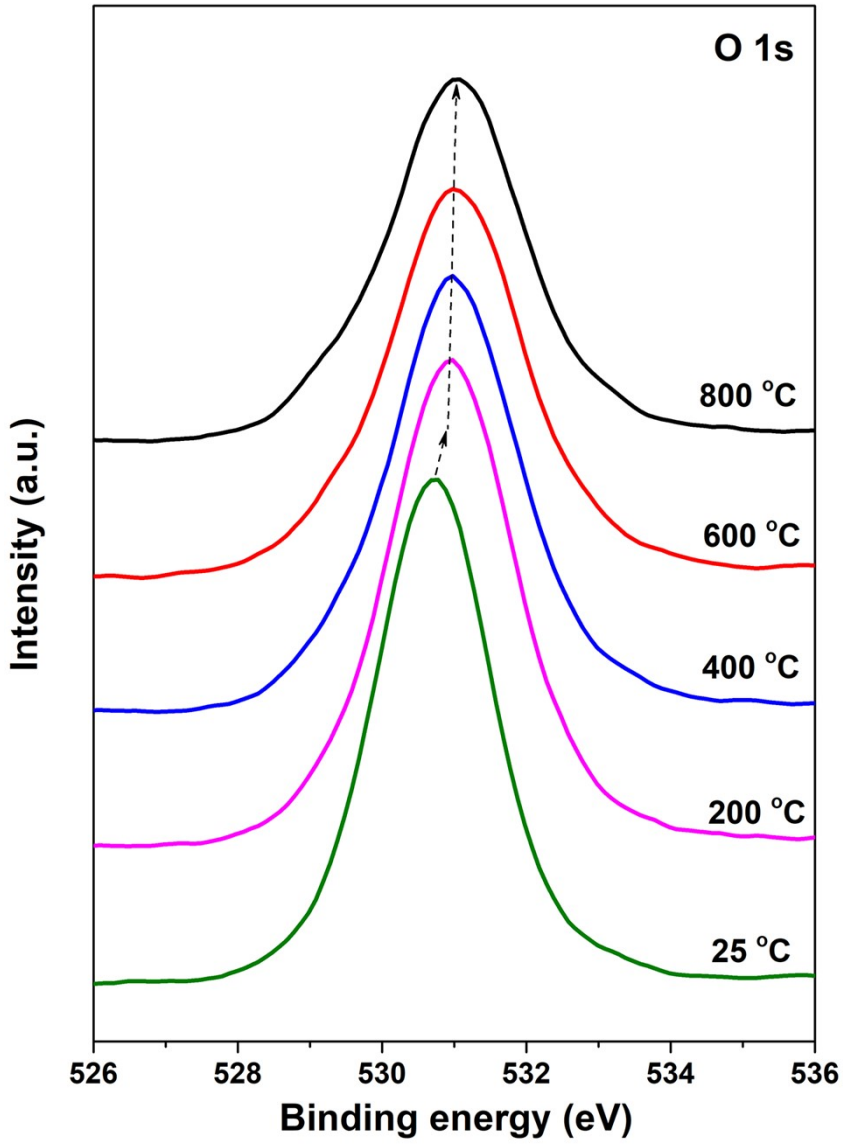

Figure S12. *In-situ* XPS O 1s spectra recorded during the preparation of CoFe-NP||SA/NCFC.

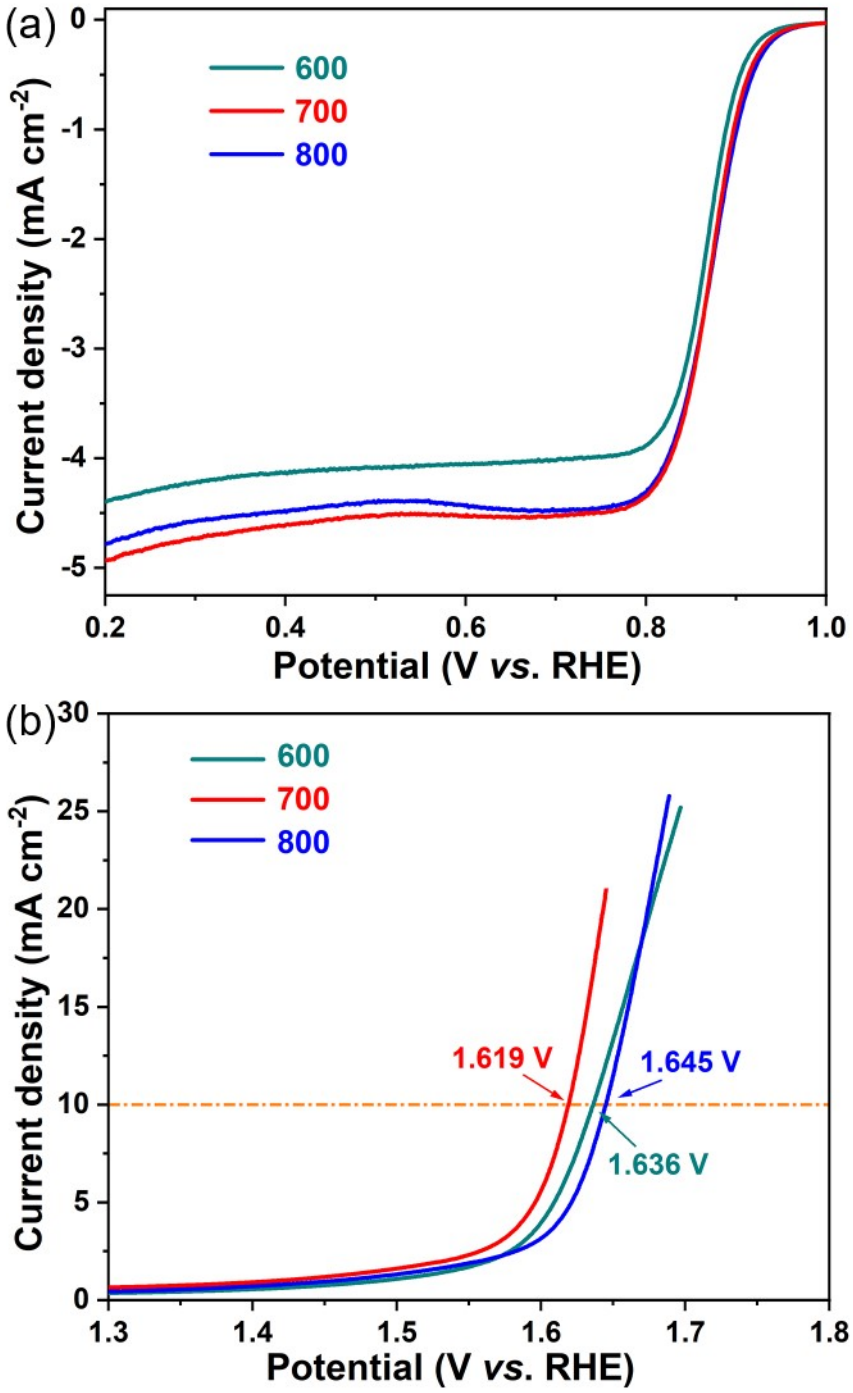

Figure S13. (a) ORR and (b) OER polarization curves of the CoFe-NP||SA/NCFC samples prepared at different thermal temperatures.

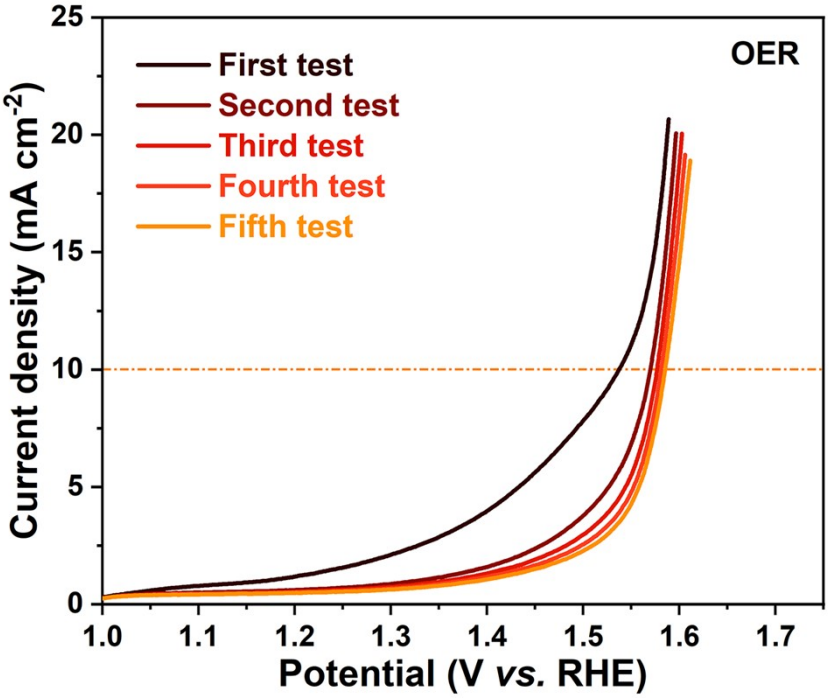

Figure S14. OER polarization curves of the CoFe-NP||SA/NCFC samples prepared under NH_3 atmospere.

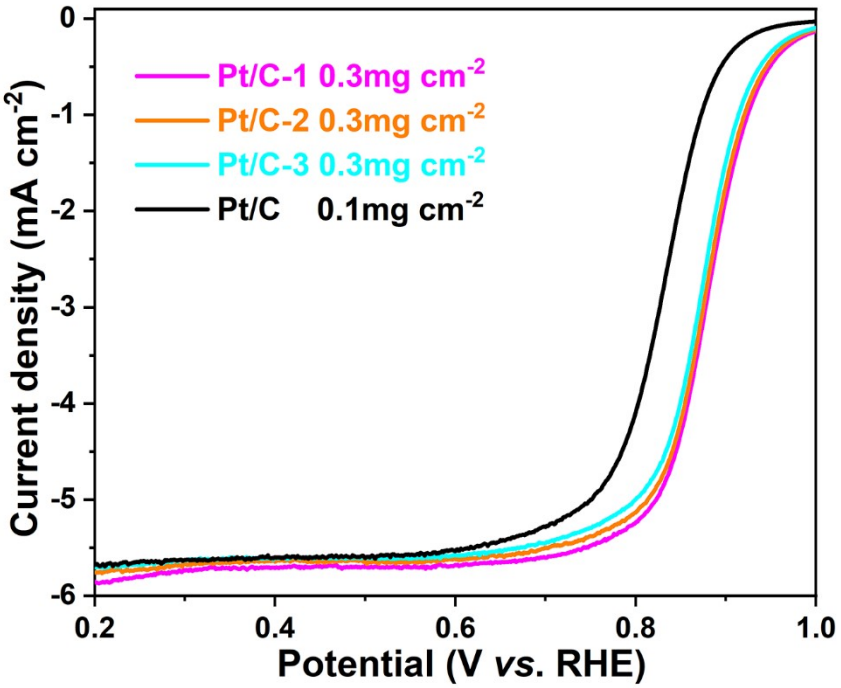

Figure S15. ORR polarization curves for Pt/C.

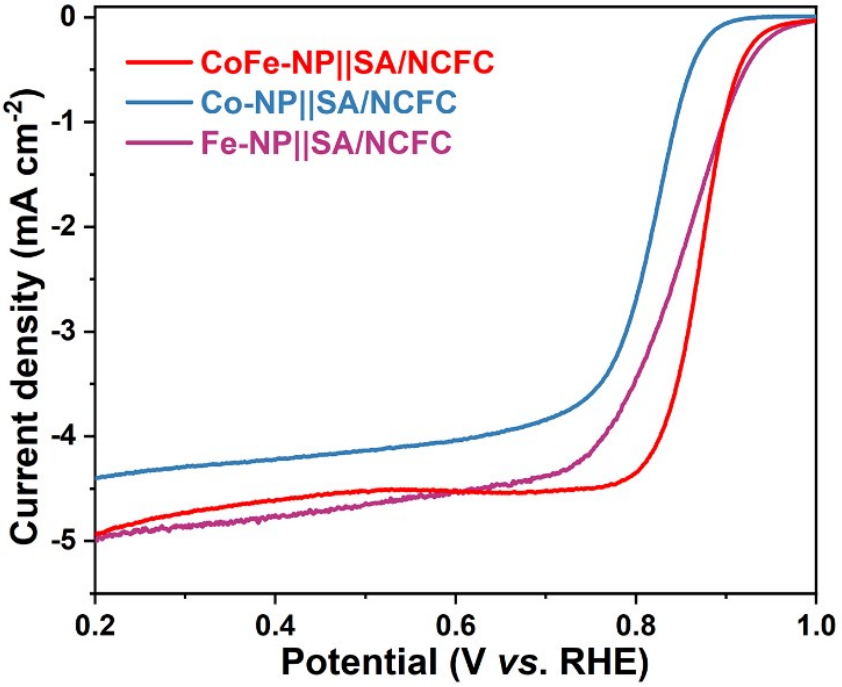

Figure S16. ORR polarization curves for CoFe-NP||SA/NCFC, Co-NP||SA/NCFC and Fe-NP||SA/NCFC.

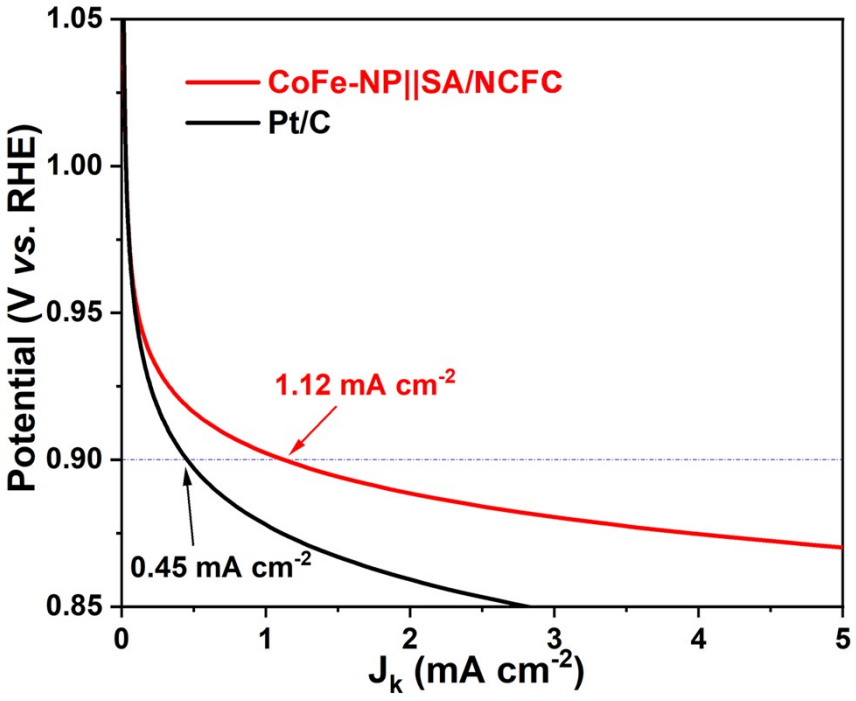

Figure S17. Kinetic current density curves of CoFe-NP||SA/NCFC and Pt/C for ORR derived from mass transport correction.

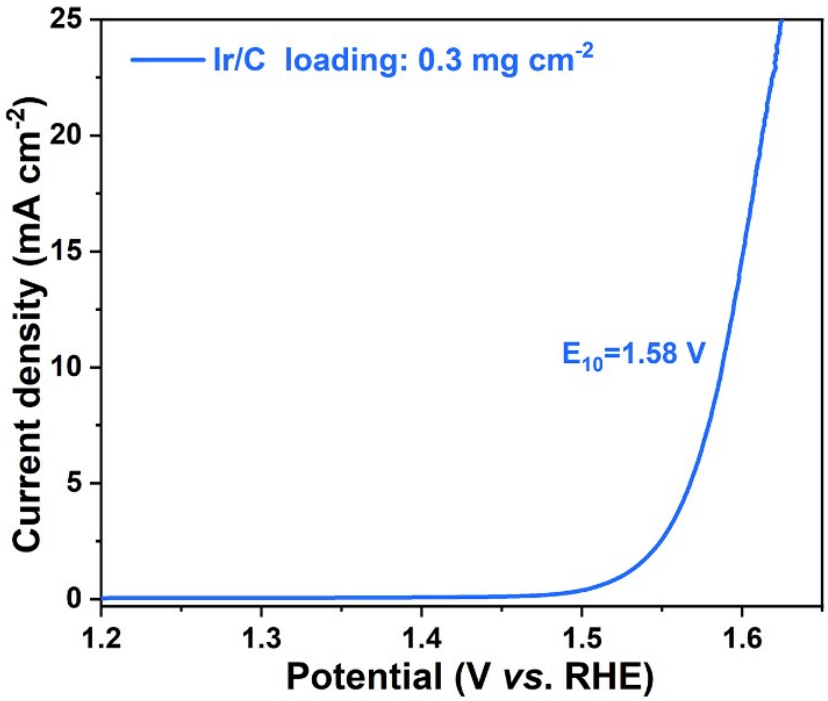

Figure S18. OER polarization curve of Ir/C with a loading of 0.3 mg cm^{-2}.

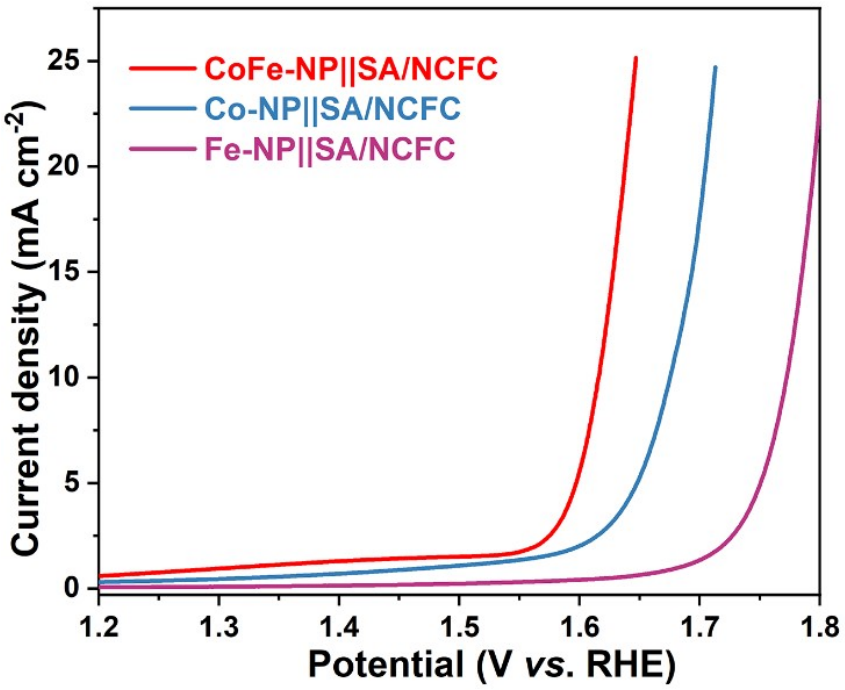

Figure S19. OER polarization curves for CoFe-NP||SA/NCFC, Co-NP||SA/NCFC and Fe-NP||SA/NCFC.

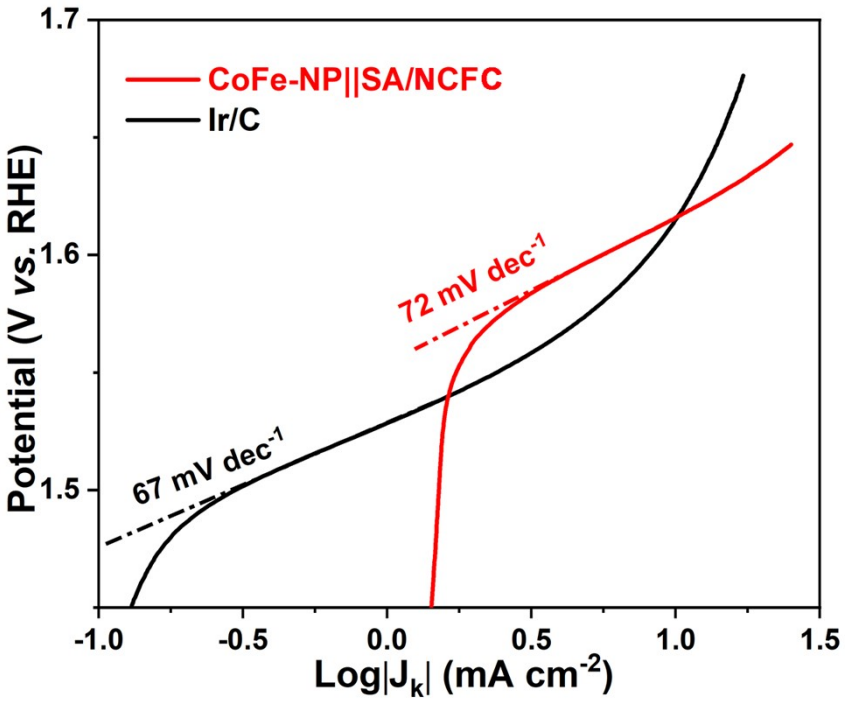

Figure S20. Tafel plots of CoFe-NP||SA/NCFC and Ir/C for OER.

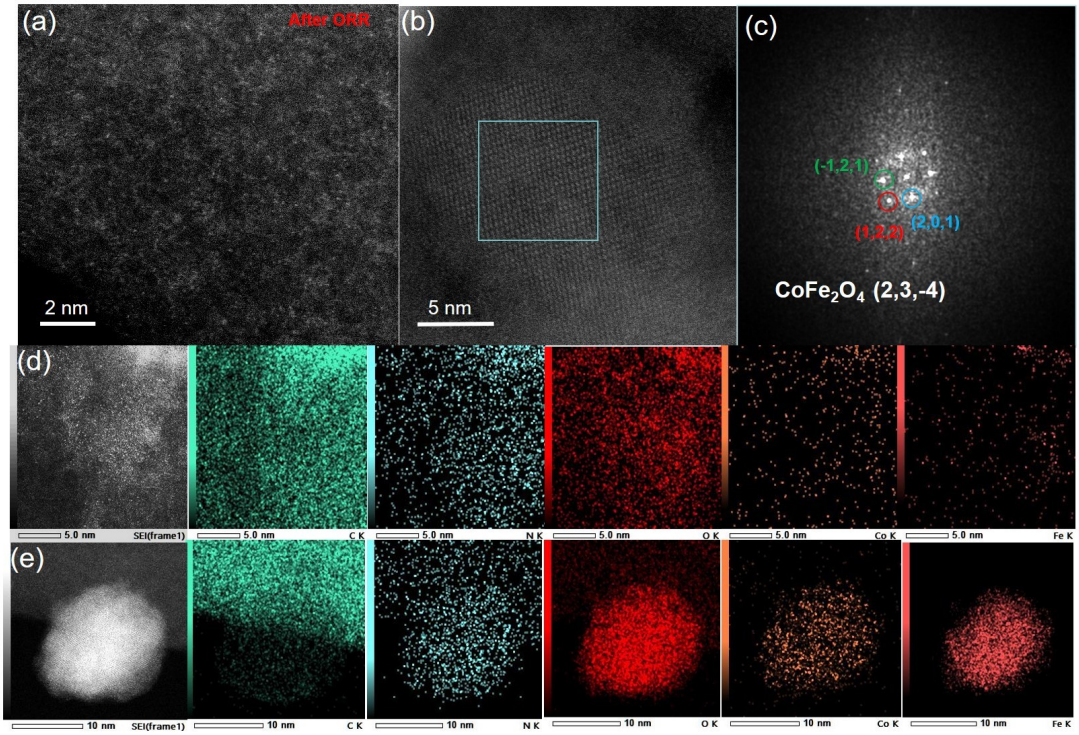

Figure S21. TEM images and EDS mapping of CoFe-NP||SA/NCFC after the ORR testing.

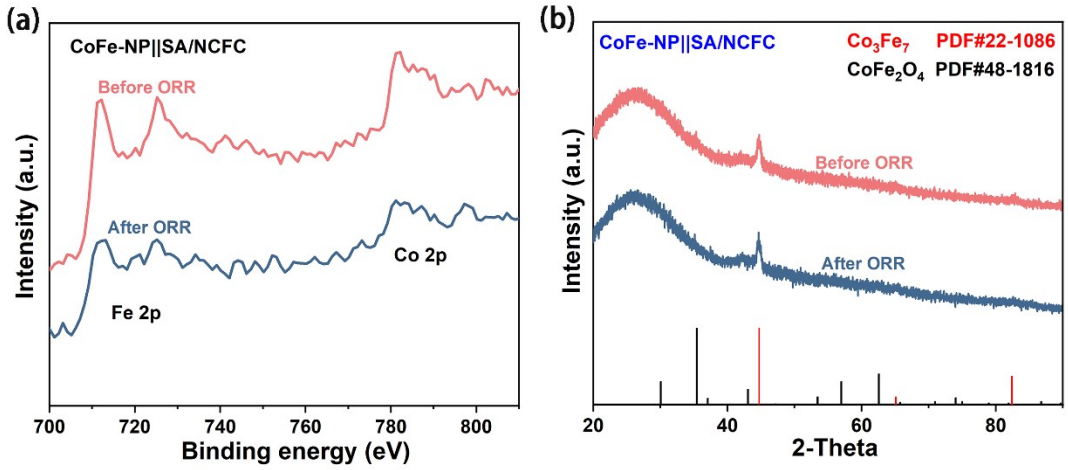

Figure S22. Comparison of (a) XPS spectra and (b) XRD patterns of CoFe-NP||SA/NCFC before and after ORR testing.

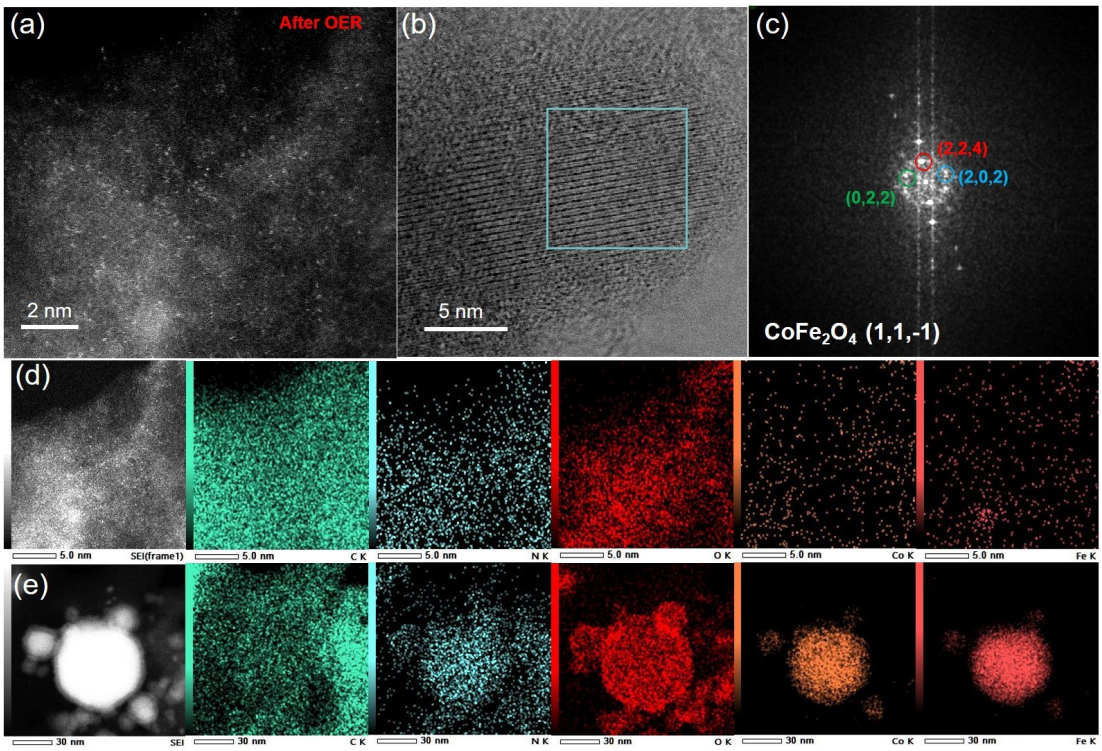

Figure S23. TEM images and EDS mapping of CoFe-NP||SA/NCFC after the OER testing.

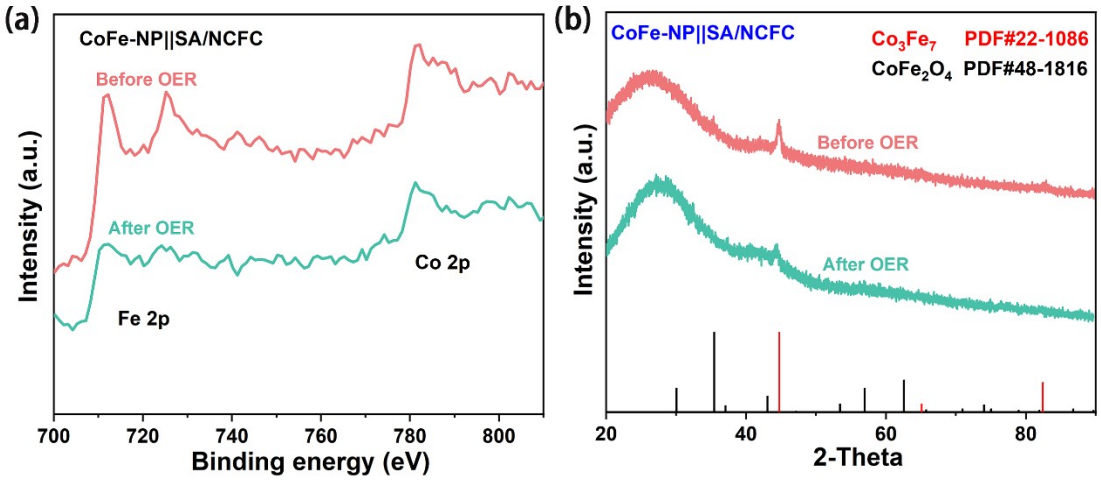

Figure S24. Comparison of (a) XPS spectra and (b) XRD patterns of CoFe-NP||SA/NCFC before and after OER testing.

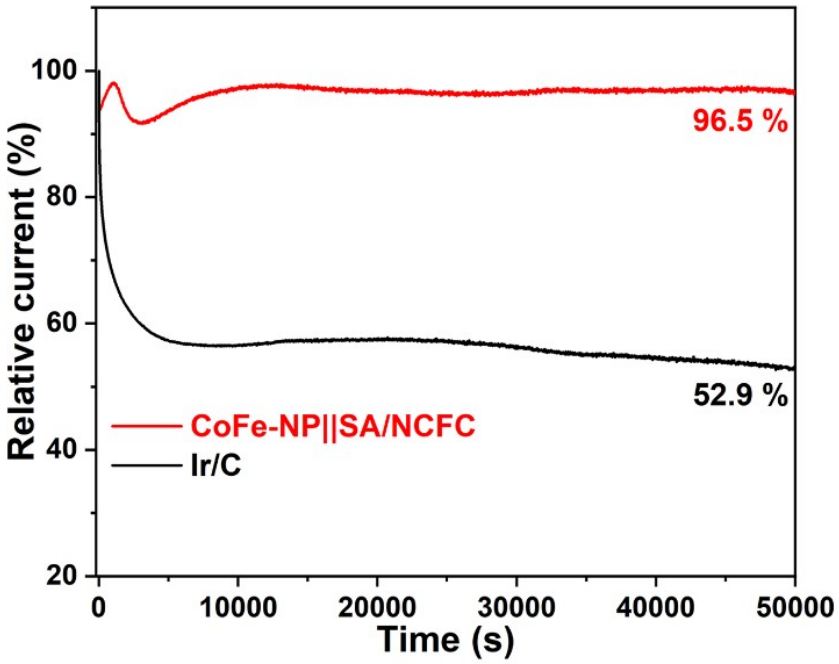

Figure S25. i-t curves of CoFeNP||SA/NCFC and Ir/C at the OER potential with 10 mA cm^{-2}.

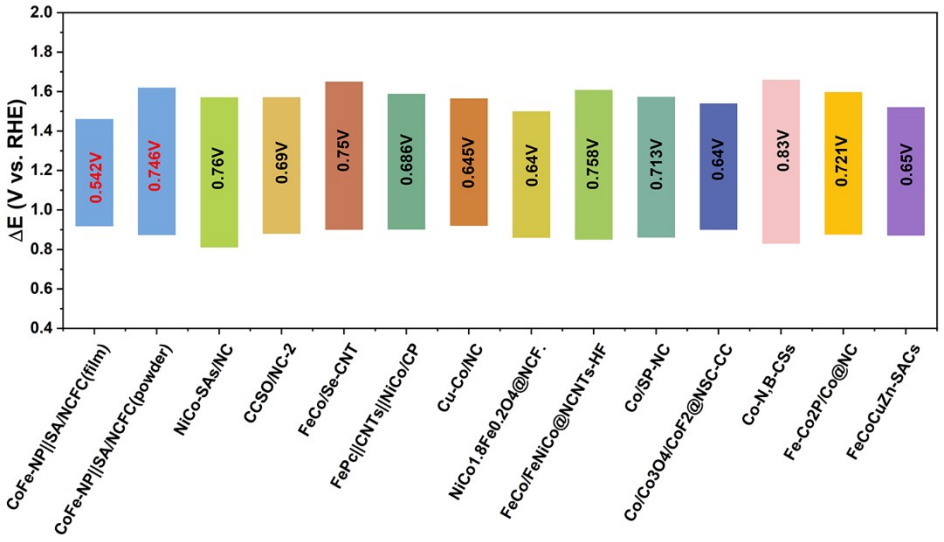

Figure R26.A comparison of oxygen electrocatalytic performance between CoFe-NP||SA/NCFC and previously reported representative catalysts.

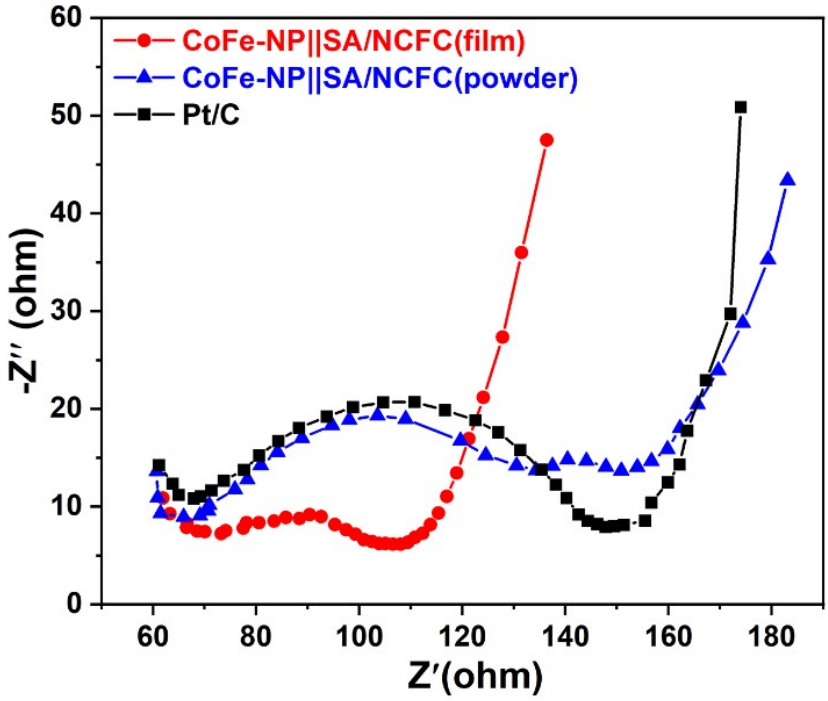

Figure S27. Electrochemical impedance spectra of CoFeNP||SA/NCFC(film), CoFeNP||SA/NCFC(powder), and Pt/C.

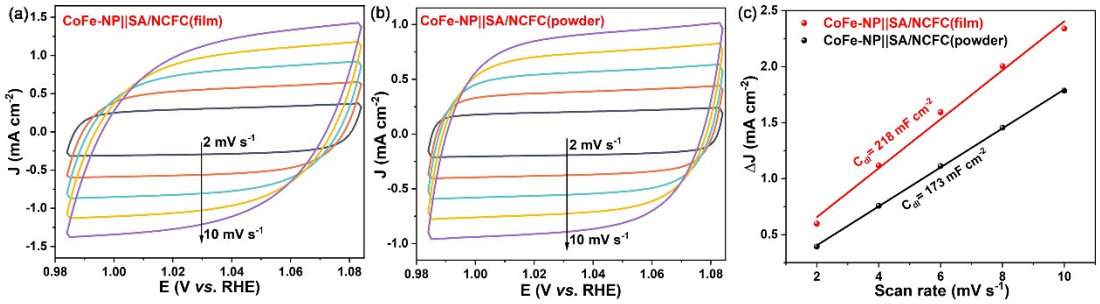

Figure S28. CV curves of (a) CoFeNP||SA/NCFC(film) and (b) CoFeNP||SA/NCFC(powder) at different scan rates. (c) Fitted line of current density difference (ΔJ) and scan rate.

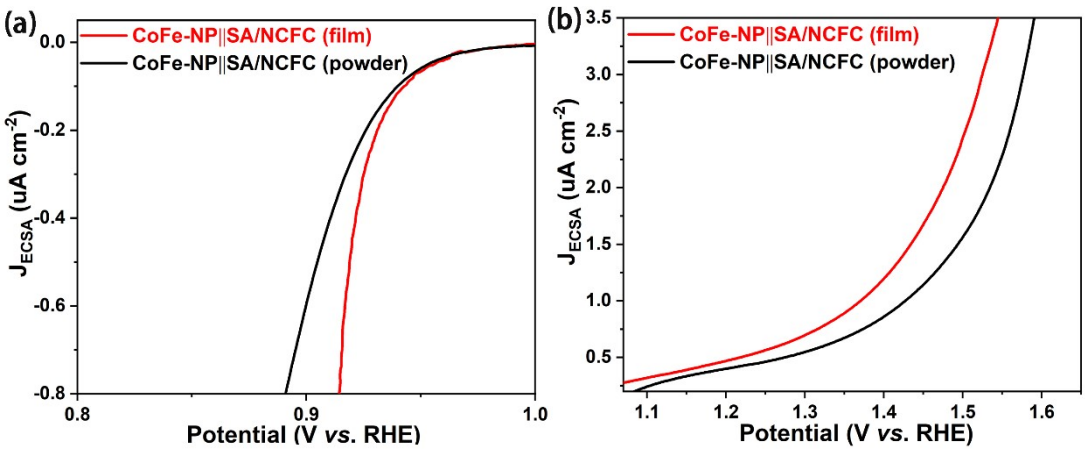

Figure S29. ECSA normalized polarization curves of CoFeNP||SA/NCFC film and CoFeNP||SA/NCFC powder.

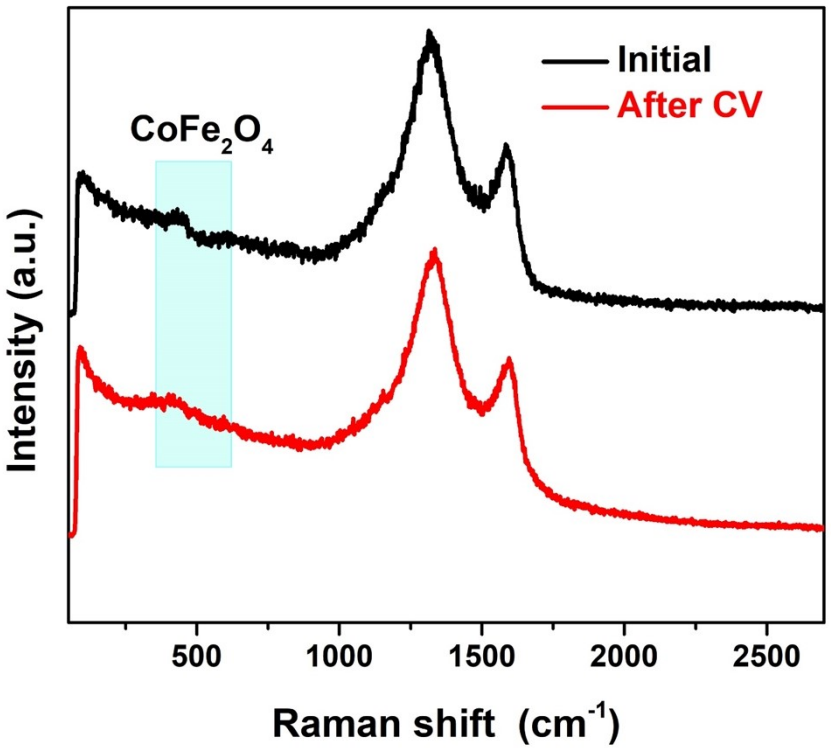

Figure S30. Raman spectra collected from CoFe-NP||SA/NCFC film before and after OER potential cycling (0.964 V-1.964 V, sweep segments: 11) in 0.1 M KOH solution.

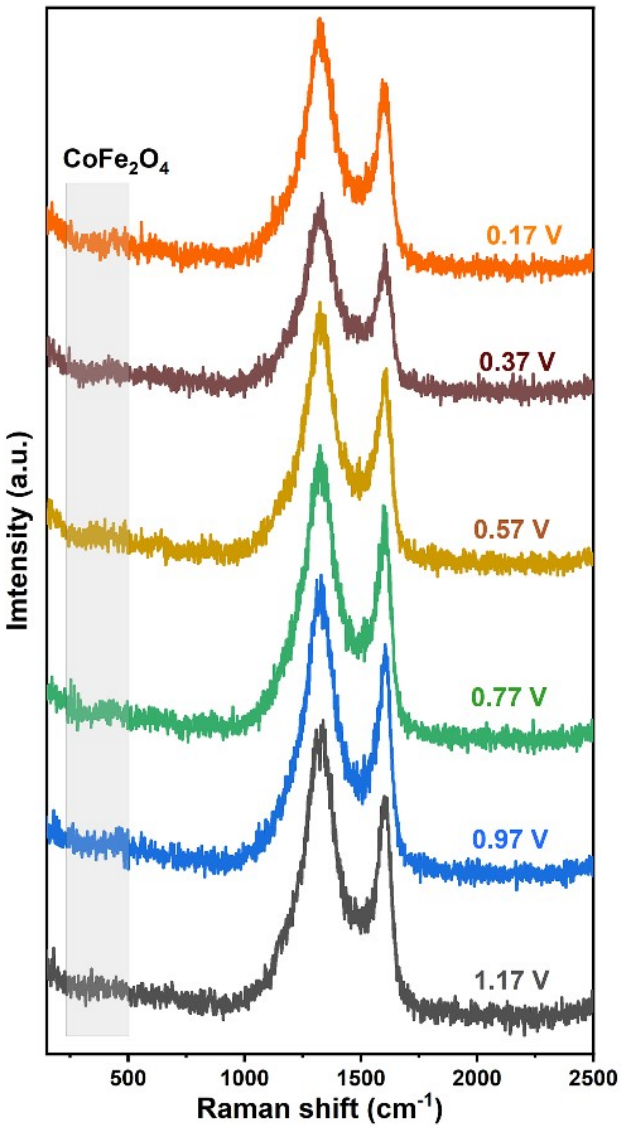

Figure S31. *In situ* Raman spectra collected from CoFe-NP||SA/NCFC film for ORR.

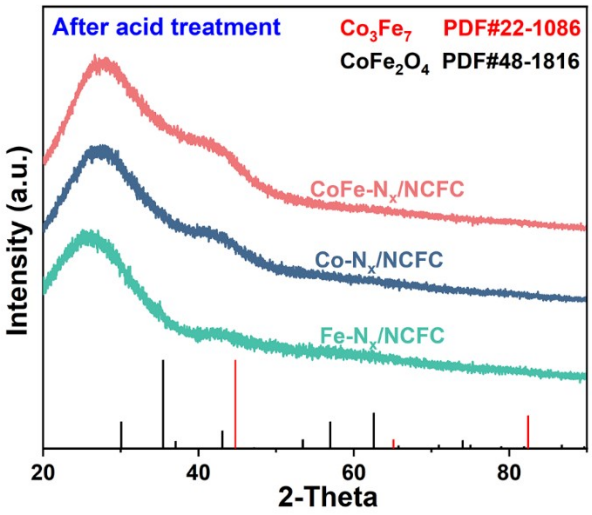

Figure S32. XRD patterns of CoFe-N_x/NCFC, Co-N_x/NCFC and Fe-N_x/NCFC prepared by acidic leaching of CoFe-NP||SA/NCFC, Co-NP||SA/NCFC and Fe-NP||SA/NCFC.

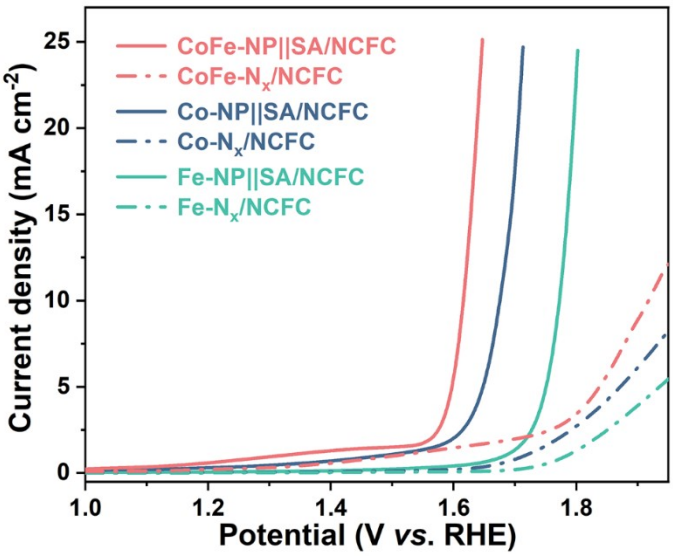

Figure S33. Comparison of OER performance of CoFe-NP||SA/NCFC, Co-NP||SA/NCFC, Fe-NP||SA/NCFC and the corresponding contrast samples of CoFe-N_x/NCFC, Co-N_x/NCFC and Fe-N_x/NCFC prepared by acid washing.

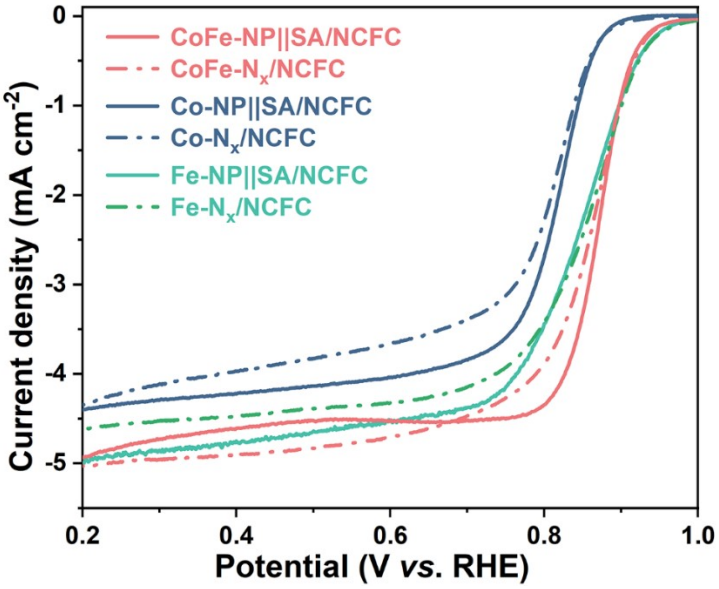

Figure S34. Comparison of ORR performance of CoFe-NP||SA/NCFC, Co-NP||SA/NCFC, Fe-NP||SA/NCFC and the corresponding contrast samples of CoFe-N_x/NCFC, Co-N_x/NCFC and Fe-N_x/NCFC prepared by acid washing.

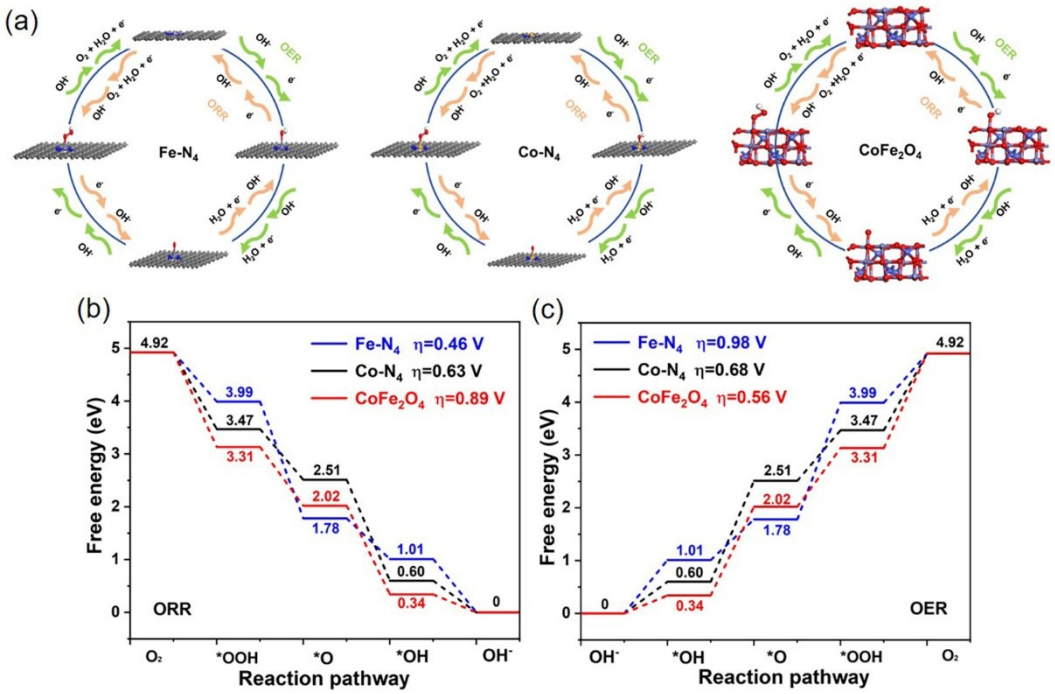

Figure S35. Free energy diagrams of the ORR and OER processes on Fe-N_4, Co-N_4 and $CoFe_2O_4$ models at U = 0 V, pH = 13, and T = 298 K. References: Adv. Funct. Mater. 2024, 34, 2314554; Carbon, 2024, 219, 118847.

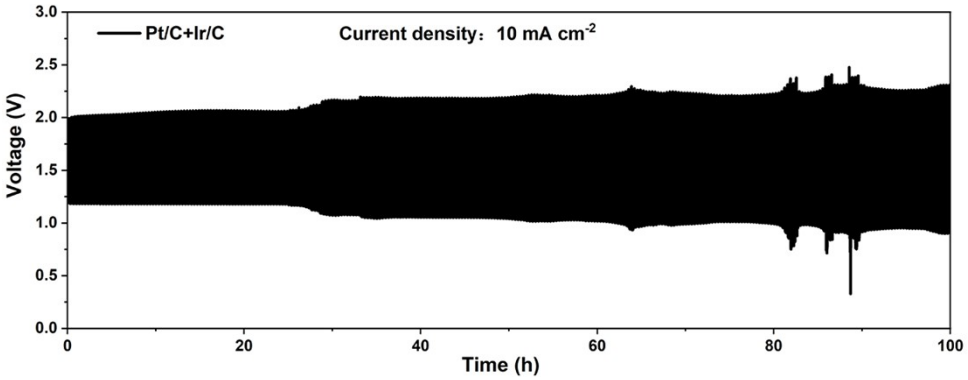

Figure S36. Galvanostatic charge-discharge cycling curve of Pt/C + Ir/C based liquid-state ZAB at 10 mA cm^{-2}.

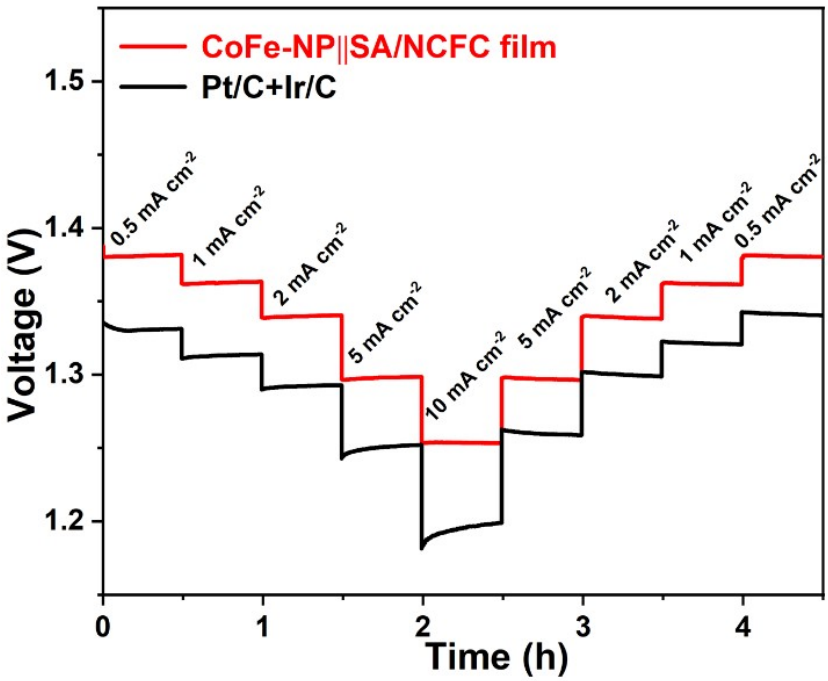

Figure S37. Discharge curves of flexible solid-state ZAB with current densities ranging from 0.5 to 10 mA cm^{-2}.

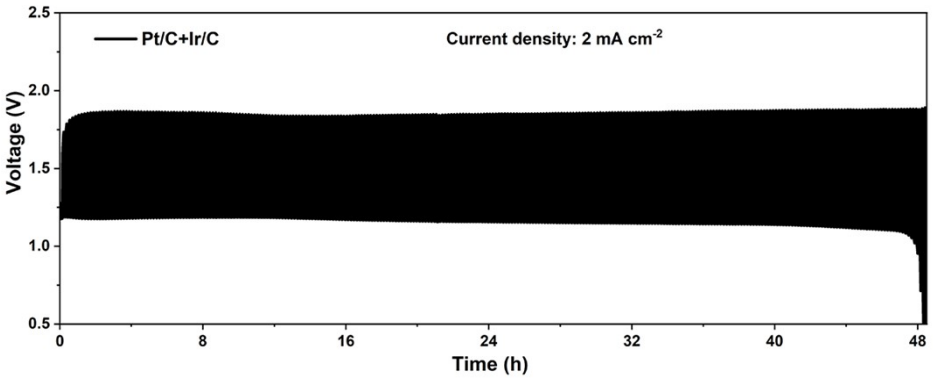

Figure S38. Galvanostatic charge-discharge cycling curves of Pt/C + Ir/C based solid-state ZABs at 2 mA cm^{-2}.

Table S1. Fe and Co contents in the CoFe-NP||SA/NCFC samples detected by ICP-MS.

Treatment temperatures	Fe content (wt.%)	Co content (wt.%)
600	10.8	7.37
700	10.3	6.43
800	5.26	3.84

Table S2. A performance comparison of constructed liquid-state ZABs between our CoFe-NP||SA/NCFC film and previously reported advanced bifunctional catalysts.

Electrocatalyst	**Power density (mW cm^{-2})**	**Cycling condition (mA cm^{-2})**	**Cyclability evaluation**	**Reference**
FeCo/Se-CNT	173.4	5	210 cycles (70 h)	Nano Lett. **2021**, 21, 2255-2264
Fe/OES	186.8	5	400 cycles (130 h)	Angew. Chem. Int. Ed. **2020**, 132, 7454
Co/Co–N–C	132	10	1000 cycles	Adv. Mater. **2019**, 31, 1901666
Fe,Co-SA/CS	86.65	5	300 cycles (100 h)	Small Methods, **2020**, 5, 2000751
ODAC–CoO–30	128.5	5	450 cycles	Adv. Funct. Mater. **2021**, 31, 2101239
Se doped MOF CoS2 HSs@CC	156.24	5	100 h	Appl. Catal. B **2023**, 330. 122523
$FeCl_3$–$NiCl_2$–GIC–73	152	5	480 cycles	Small **2022**, 18, 2107667
Fe/SNCFs-NH_3	255.84	1	1000 cycles (1000 h)	Adv. Mater. **2022**, 34, 2105410
CoFe-NP||SA/NCFC film	237.4	10	2300 cycles (770h)	This work

Table S3. A performance comparison of constructed solid-state ZABs between our CoFe-NP||SA/NCFC film and previously reported advanced bifunctional catalysts.

Electrocatalyst	**Open Voltage (V)**	**Peak power density (mW cm^{-2})**	**Cyclability evaluation**	**Reference**
FeCo/Se-CNT	1.405	37.5	**---**	Nano Lett. **2021**, 21, 2255-2264
Fe/SNCFs-NH_3	1.34	---	120 cycles	Adv. Mater. **2022**, 34, 2105410
Ni/N-ESC	1.43	144.1	500 cycles	Energy Storage Mater. **2022**, 47, 235–248
Fe_1/d-CN	1.2	~80	20 h	Energy Environ. Sci., **2021**, 14, 6455–6463
NGM-Co	1.439	~30	---	Adv. Mater. **2017**, 29, 1703185
Co@C–O–Cs	1.434	59.1	---	Nano Micro Lett. **2023**, 15, 28
Co_4N@d-NCNWs/D	1.41	26.5	28 h	Adv. Energy Mater. **2023**, 2301749
Fe SA/NCZ	1.447	101	44 h	Adv. Funct. Mater. **2023**, 33, 2213897
CoFe-NP||SA/NCFC film	1.5	141.1	73 h	This work